

**FULL PAPER**

Synthesis of ferrocenyl-containing silicone rubbers via platinum-catalyzed Si–H self-cross-linking

Konstantin V. Deriabin¹ | Ekaterina K. Lobanovskaya¹ | Sergey O. Kirichenko¹ | Marie N. Barshutina² | Pavel E. Musienko² | Regina M. Islamova¹

¹ Institute of Chemistry, Saint Petersburg State University, 7/9 Universitetskaya Naberezhnaya, Saint Petersburg, Russia, 199034

² Institute of Translational Biomedicine, Saint Petersburg State University, 7/9 Universitetskaya Naberezhnaya, Saint Petersburg, Russia, 199034

Correspondence

Islamova R. M., Institute of Chemistry, Saint Petersburg State University, 7/9 Universitetskaya Nab., Saint Petersburg, Russia, 199034.
Email: r.islamova@spbu.ru

Funding information

Russian Foundation for Basic Research, Grant/Award Number: 18-33-20062_mol_a_ved

Self-cross-linkable ferrocenyl-containing polymethylhydrosiloxanes were synthesized. Karstedt's catalyst and *cis*-[PtCl₂(BnCN)₂] were examined as cross-linking catalysts at room temperature for the reaction between Si–H groups of the ferrocenyl-containing polymethylhydrosiloxanes. *Cis*-[PtCl₂(BnCN)₂] is an effective catalyst that allows cross-linked ferrocenyl-containing silicones (silicone rubbers) to be obtained with *no visible* mechanical defects (bubbles or cracks) compared with Karstedt's catalyst. The ferrocene content of the ferrocenyl-containing silicone rubbers was found to be approximately 50 wt.% by energy-dispersive X-ray analysis. Compared with cross-linked non-modified polymethylhydrosiloxanes, the ferrocenyl-containing silicone rubbers exhibited improved tensile properties (the tensile strength increased from 0.47 to 0.75 MPa) and a 1.5–2.5 times lower cross-linking degree. The surface resistivity of the ferrocenyl-containing silicone rubbers (50 wt.% ferrocenyl units) was approximately $7 \times 10^9 \Omega/\square$, which was 10,000 times lower than that of pure polymethylhydrosiloxane. The obtained flexible electroactive ferrocenyl-containing silicone rubbers can potentially be applied as coatings for electronic and electrostatic-sensitive devices, interfaces, and sensors.

KEYWORDS

coatings, ferrocenyl-containing polymethylhydrosiloxanes, platinum(0) and (II) catalysts, redox-active silicone rubbers, self-cross-linking

1 | INTRODUCTION

The development of flexible electroactive coatings has aroused considerable research interest owing to their promising applications as electrostatic discharge (ESD) protective materials for electrostatic-sensitive devices and power lines,^[1–10] active layers for modern sensing electronic devices,^[11–17] stretchable supercapacitors,^[16,18,19] and biomedical implants.^[17,20–22] Electroactive coatings are usually polymer composites with conductive fillers.^[1–22] The composites must be non-toxic, environmentally friendly, economical in use, and thermally and chemically stable.^[1,2]

An application of silicone composite coatings offers an excellent opportunity to meet the aforementioned requirements. Polysiloxanes are well known as excellent insulators that exhibit high flexibility and good adhesion to a wide range of substrates and possess substantial weather and biofouling resistance.^[23–27] The use of conductive fillers such as carbon nanotubes and nanofibers,^[11–13,16,20] graphite,^[10,28] graphene,^[13,15,16] metals,^[10,13,16,22] and π-conjugated polymers^[9,13,17] contributes to transforming a typical dielectric into a semiconductor (conductivity of approximately 10^2 – 10^{-10} S/cm^[10,13,16,17,22]). The fillers are applied to prevent the long-term preservation of excessive static electrical

charges, which create severe hazards in industries (such as risks of explosions),^[29] and for energy storage.^[16,18,19] The general disadvantage of these fillers is that they promote the irregular distribution of conductive particles in a silicone matrix, which leads to delamination of the polymer composite.^[30,31] Moreover, some used fillers (e.g. silicon carbide, carbon black, and graphite)^[30,31] are toxic and usually spoil the mechanical properties of the material, such as the strength and tensile elongation.^[30]

The preparation of curable silicone co-polymers that contain electroactive fragments chemically attached to a silicone backbone is of considerable demand. In addition, integrating metals into a polymer chain can influence its electronic and optical properties.^[32,33] For instance, some cyclic,^[34–37] linear,^[34,38–45] and dendritic^[34,36,46,47] oligo/polysiloxanes and silsesquioxanes.^[47,48] with redox-active ferrocenyl moieties have been synthesized. However, the ferrocenyl-containing oligosiloxanes are liquid and cannot be used as coatings and active layers for electrical devices. To address this problem, a silicone co-polymer should be cross-linked by active functional groups^[49] in its structure.

A literature survey indicated that there are no investigations into the cross-linking of ferrocenyl-containing polysiloxanes. Nevertheless, self-cross-linking was observed for hydride-containing polysiloxanes in our previous work.^[49] Hence, it is a challenging task to synthesize silicone materials that are self-cross-linkable by Si-H groups, are made electroactive by ferrocenyl moieties, and exhibit flexibility.

Thus, the general aims of this study are (i) to obtain and cross-link poly[methylhydrosiloxane-co-methyl(2-ferrocenylethyl)siloxanes] using Karstedt's catalyst and *cis*-[PtCl₂(BnCN)₂] (Bn = PhCH₂)^[24]; (ii) to investigate both the cross-linking degree by swelling measurements and the mechanical properties of the cross-linked products (silicone rubbers); (iii) to analyze the ferrocene content in the cross-linked ferrocenyl-containing polymethylhydrosiloxanes; (iv) to explore their electrical resistance by impedance measurements; and (v) to propose a possible mechanism of conductivity.

2 | EXPERIMENTAL

2.1 | Materials and methods

α,ω -Di(trimethylsiloxy)polymethylhydrosiloxane (**PMHS**) (number average molecular weight M_n = 1700–3200, viscosity 12–45 cSt, Sigma-Aldrich, St. Louis, USA), α,ω -di(dimethylvinylsiloxy)polydimethylsiloxane (**PDMS-v**) (number average molecular weight

M_n = 19,000, viscosity 850–1150 cSt, Sigma-Aldrich, St. Louis, USA) and platinum(0)-1,3-divinyl-1,1,3,3-tetramethyldisiloxane complex solution 0.1 M in xylene (abcr GmbH, Karlsruhe, Germany) were purchased from commercial suppliers and fully characterized by nuclear magnetic resonance (NMR) spectroscopy before usage. Ferrocene (Shanghai Macklin Biochemical Co., Shanghai, China), acetyl chloride, aluminum chloride, sodium carbonate, anhydrous sodium sulfate, lithium alanate, hydroquinone, blue copper sulfate, 40% hydrofluoric acid, 30% hydrogen peroxide, diethyl ether, hexane, toluene, benzene, and dichloromethane (Vekton, Saint Petersburg, Russia) were purchased from commercial suppliers and were used as received. Anhydrous solvents were freshly distilled (CH₂Cl₂ over CaH₂, Et₂O over LiAlH₄, and benzene over Na/benzophenone). Copper sulfate was thermally dehydrated. *Cis*-[PtCl₂(BnCN)₂] and vinylferrocene were prepared according to the published methods^[50–52] (see Supporting Information; Figures S2 and S3).

Thin-layer chromatographic analysis was carried out on silica gel chromatography plates (Macherey-Nagel ALUGRAM UV254; sorbent: silica 60, specific surface area 500 m²/g, mean pore size 60 Å, specific pore volume 0.75 ml/g, particle size 5–17 mm; binder: highly polymeric product, which is stable in almost all organic solvents and resistant to aggressive reagents). Column chromatography was performed on silica gel (0.04–0.063 mm, 60 Å, CAS 7631-86-9) and on neutral aluminum oxide (LL 5/40, Vekton, CAS 1344-28-1). NMR spectra were recorded on Bruker AVANCE III 400 spectrometers in CDCl₃ at 25 °C (at 400 MHz for ¹H, 100 MHz for ¹³C, 80 MHz for ²⁹Si NMR spectra, respectively). Chemical shifts are given in δ-values (ppm) referenced to the residual signals of non-deuterated solvent (CHCl₃): δ 7.26 (¹H) and 77.2 (¹³C). For ¹H NMR, the resonance multiplicity was described as s (singlet), d (doublet), t (triplet), and m (multiplet). Solid-state NMR (SSNMR) spectra were obtained using a Bruker AVANCE III 400-MHz WB (three-channel SSNMR spectrometer with magnetic resonance imaging/diffusion capability) operating at 400.23 MHz for ¹H (16 scans), 100.64 MHz for ¹³C (2000 scans), and 79.51 MHz for ²⁹Si (2000 scans) under magic-angle spinning conditions with spin rates of approximately 12,500 Hz. ¹³C and ²⁹Si SSNMR spectra were recorded with cross-polarization (typically with a recycle delay of 2 s and a contact time of 2.0 ms) and direct excitation (typically with a recycle delay of 5 s) with ¹H decoupling. ¹H spectra were obtained with direct excitation. Samples were run as prepared, and spectral referencing was performed with respect to external, neat tetramethylsilane. Tension tests were carried out on a

Shimadzu EZ-L-5kN universal testing machine at a constant cross-head speed of 50 mm/min (tension testing of samples). Surface resistivity measurements were performed with a Mitsubishi Hiressta-UP MCP-450HT electrometer using standard ring-shaped URS probes with samples prepared via the aforementioned method. At least three measurements were made on each sample; the final readings were performed 10 s after 1000-V voltage application.

2.2 | Synthesis of α,ω -trimethylsiloxy poly[methylhydrosiloxane-co-methyl(2-ferrocenyl-ethyl)siloxane]

Ferrocenyl-containing polymethylhydrosiloxane with Karstedt's catalyst (FS1). Vinylferrocene (1.5 g, 7.08 mmol) was added to a benzene solution (10 ml) containing 20 μ l of a 0.1 M solution of Karstedt's catalyst in xylene in a tube under argon atmosphere. The mixture was stirred at room temperature (RT) for approximately 1 hr. A gentle stream of argon was blown through the solution for a few seconds. A solution of PMHS (849 mg, 14.15 mmol of $-\text{OSiHCH}_3-$ units) in dry benzene (10 ml) was added dropwise over a period of 1 hr. The contents of the tube were sealed and stirred at 40 °C for 24 hr. During this time, the original orange color of the solution darkened to orange brown. The solvent was removed under reduced pressure. Yield: 100%; brown viscous liquid. ^1H NMR (400 MHz, CDCl_3 , δ , ppm): 0–0.40 (broad s, CH_3Si), 0.90 (broad, 2H, $-\text{CH}_2\text{CH}_2-$), 2.41 (broad, 2H, $-\text{CH}_2\text{CH}_2-$), 4.00–4.30 (broad, 9H, **Cp**, C_5H_4), 4.83 (broad s, 1H, Si-**H**). The ^1H NMR spectra showed that the molar content of $-\text{OSiHCH}_3-$ units was approximately 50% (Figure S7, Supporting Information). ^{13}C NMR (100 MHz, CDCl_3 , δ , ppm): 0–2.5 (CH_3Si), 18.8 ($\equiv\text{SiCH}_2\text{CH}_2\text{Cp}_2\text{Fe}$), 22.7 ($\equiv\text{SiCH}_2\text{CH}_2\text{Cp}_2\text{Fe}$), 67.7 (3,4-**Cp** CH_2CH_2-), 68.1 (2,5-**Cp** CH_2CH_2-), 69.1 (**Cp**), 92.7 (ipso **Cp**) (Figure S8, Supporting Information). ^{29}Si NMR (80 MHz, CDCl_3 , δ , ppm): -37 ($-\text{OSiHCH}_3-$), -22 [- $\text{OSi}(\text{CH}_3)(\text{CH}_2\text{CH}_2\text{Cp}_2\text{Fe})-$], 10 (end groups $[\text{CH}_3]_3\text{Si}-$) (Figure S9, Supporting Information).

Ferrocenyl-containing polymethylhydrosiloxane with cis-[PtCl₂(BnCN)₂] (FS2) was synthesized using the same method described earlier for **FS1**. The differences are (i) the use of *cis*-[PtCl₂(BnCN)₂] (20 μ l of 0.1 M *cis*-[PtCl₂(BnCN)₂] in dichloromethane) instead of Karstedt's catalyst (20 μ l of 0.1 M Karstedt's catalyst in xylene) and (ii) dichloromethane as a solvent instead of benzene.

2.3 | General cross-linking procedure

The concentrated solution of **FS1** (500 mg) in benzene or **FS2** (500 mg) in dichloromethane was poured into a polytetrafluoroethylene mold measuring 36 mm length \times 14 mm width \times 3 mm height and dried at RT for 12 hr followed by drying at 80 °C for 5 hr. Cross-linked products were obtained: ferrocenyl-containing silicone rubber with Karstedt's catalyst (**FSR1**) and ferrocenyl-containing silicone rubber with *cis*-[PtCl₂(BnCN)₂] (**FSR2**). The final concentration of the catalysts in **FSR1** and **FSR2** was 10⁻³ M.

The preparation of the cross-linked **PMHS**, catalytic hydrosilylation cross-linking of **FS1/PDMS-v** and **FS2/PDMS-v** mixtures, preparation of ferrocene-**PMHS** mixtures (Figure S1), the procedures for density determination and swelling measurements are described in the Supporting Information (see the “Experimental” section).

2.4 | Impedance measurements

Samples for electrical conductivity measurements were prepared in the form of round plates with a fixed diameter of 30 mm and thickness from 0.2 to 0.4 mm. The sample of liquid polysiloxane was cross-linked on one round plate via the procedure described earlier followed by 10-nm carbon film thermal sputtering in Quorum Technologies Q150 TES sputter coater to ensure full surface contact. The samples were then covered with a second gold-plated brass electrode in a sandwich structure. The measurements of alternating current-specific electrical conductivity were performed with a Novocontrol Alpha Broadband Dielectric spectrometer and a BDS1100 shielded sample cell providing constant clamping pressure to sample the sandwich structure. The temperature of the sample plate was adjusted by evaporated liquid nitrogen flowing through gas heaters. The precision of the temperature control was better than 0.1 °C, and the samples were allowed to reach thermal equilibrium before the conductivity experiment for at least 300 s at 20 °C. The measurement sequence included a frequency sweep (1000.0–0.1 Hz; 10 points per decade) with 30-mV signal amplitude. At least five meterings were made per frequency step followed by median-specific resistance averaging.

Broadband dielectric spectroscopy was used to study the details of the conductivity mechanisms in **FSR2**. However, in conductive polymer systems, the presence of impurities, electrode polarization, and space charge separation phenomena usually lead to distortion or even full obscuration of relaxation peaks in the ε^* (complex dielectric permittivity) representation. To overcome such difficulties, it was decided to use the electric modulus

formalism, which is extensively used to interpret conductivity effects in ionic and polymeric conjugated conductors^[53,54] even despite divergent views regarding its applicability.^[55,56] The electric modulus (M^*) is defined as the inverse complex function of dielectric permittivity and is given as follows:

$$M^* = \frac{1}{\varepsilon^*} = \frac{\varepsilon'}{\varepsilon'^2 + \varepsilon''^2} + i \frac{\varepsilon''}{\varepsilon'^2 + \varepsilon''^2} = M' + iM'' \quad (1)$$

The use of this approach focuses on the study of electric field E relaxation under constant displacement vector D rather than revealing D relaxations with small constant field E in the classic dielectric permittivity method. This approach has two advantages in the investigation of systems with mobile charges: (i) it allows low-frequency electrode effects to be overwhelmed and allows focus on small changes against large effects on the background; and (ii) the electric conductivity relaxation is separated into individual peaks in the M'' versus frequency plot. Because the real and imaginary parts of the complex modulus function are interrelated via Kramers–Kronig relations, we concentrate on investigating the imaginary part M'' as a more convenient representation.

3 | RESULTS AND DISCUSSION

3.1 | Cross-linking of the ferrocenyl-modified PMHSs and NMR characterizations

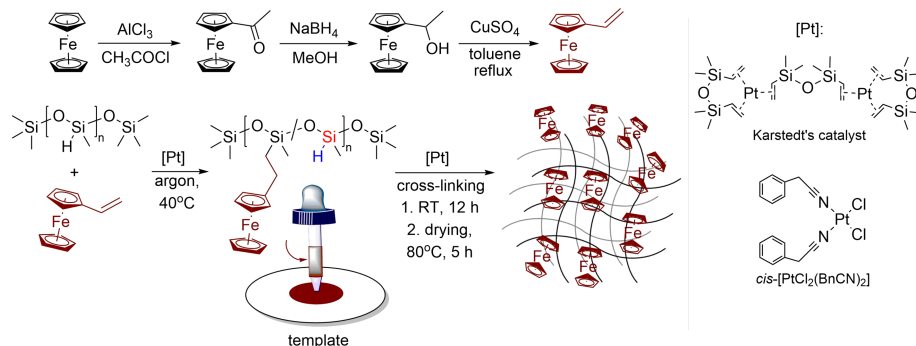
FS1 and **FS2** were synthesized by catalytic hydrosilylation between **PMHS** and vinylferrocene (Scheme 1). The molar ratio of the Si–H groups and vinylferrocene was selected so that 50% of the hydride Si–H groups remained unreacted. **FS1** and **FS2** were analyzed by ^1H , ^{13}C , and ^{29}Si NMR spectroscopy and compared with **PMHS** and vinylferrocene (Figures S2–S9, Supporting Information). The ^1H NMR spectra of **FS1** and **FS2** showed two peaks at δ 0.90 ppm and 2.41 ppm,

corresponding to $\text{Cp}_2\text{FeCH}_2\text{CH}_2\text{Si}\equiv$ (Figure S7, Supporting Information). ^{29}Si NMR analysis of **FS1** and **FS2** showed a new single peak at –22 ppm corresponding to 2-ferrocenylethyl-substituted silicon $\text{Cp}_2\text{FeCH}_2\text{CH}_2\text{Si}\equiv$ (Figure S9, Supporting Information).

The self-cross-linking of **FS1** and **FS2** was carried out at RT for 12 hr, followed by drying of the cured rubber at 80 °C for 5 hr on a template (Scheme 1). The obtained **FSR1** and **FSR2** were characterized by non-tackiness, a red-brown color, and distinct flexibility (Figure 1). The concentrations of both catalysts were 10^{-3} M. **FSR1** and **FSR2** were analyzed by ^1H , ^{13}C , and ^{29}Si SSNMR spectroscopy (Figures S10–S15, Supporting Information) and compared with **FS1** and **FS2** (Figures S7–S9, Supporting Information). The ^{29}Si SSNMR spectra of **FSR1** and **FSR2** showed new peaks at –26 ppm corresponding to Si–Si^[57] and at –56 ppm and –66 ppm corresponding to O-trisubstituted silicon atoms^[49,57,58] (Figures S12, S15, Supporting Information). The self-cross-linking of **FS1** and **FS2** is possibly similar to that of **PMHS**^[49] (Figures S16–S21, Supporting Information) and takes place through platinum-catalyzed Si–Si dehydrocoupling^[49,59,60] and autoxidation of Si–Si bonds in air^[49,59–61] (Scheme 2).

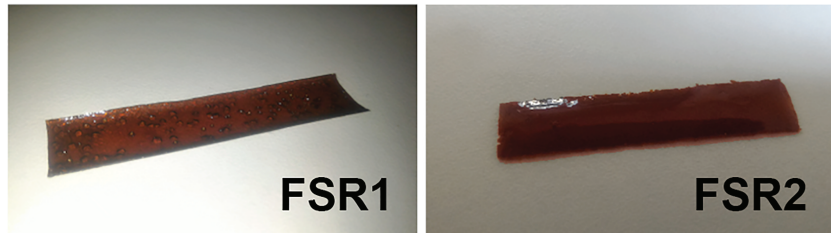
In contrast to **FSR1**, **FSR2** is a red-brown transparent and smooth material with no visible structural defects, such as bubbles and cracks (Figure 1). Karstedt's catalyst demonstrates higher activity than does *cis*-[PtCl₂(BnCN)₂], resulting in premature cross-linking. This result is in good agreement with our previous studies.^[23,24,27,49] The *bis*-nitrile platinum(II) complex is obtained according to the well-known published method^[50,51] and is soluble in chloroorganic solvents such as CH₂Cl₂ and CHCl₃. *cis*-[PtCl₂(BnCN)₂] is a more shelf-stable and moisture/air-insensitive and less active platinum(II) complex than Karstedt's catalyst. These facts make *cis*-[PtCl₂(BnCN)₂] a preferable alternative to Karstedt's catalyst in the cross-linking of the observed ferrocenyl-containing polysiloxanes.

The preparation of ferrocenyl-containing silicone rubbers by a “classical” two-component hydrosilylation



SCHEME 1 Schematic displaying the stepwise procedure for the synthesis of the ferrocenyl-containing silicone rubbers.

FIGURE 1 Photos of ferrocenyl-containing silicone rubbers with Karstedt's catalyst (**FSR1**) and with *cis*-[PtCl₂(BnCN)₂] (**FSR2**)



approach (using **FS1** or **FS2** and **PDMS-v**) was unsuccessful due to poor miscibility of the ferrocenyl-containing and vinyl-containing components, which leads to low-quality (defective and heterogeneous) rubbers with a lower ferrocene content than in **FSR1** and **FSR2**.

Consequently, the reactions between Si–H groups represent a new cross-linking method for polysiloxanes^[49] that provides the opportunity to use one-component silicone curing systems at RT. It can also be used whenever the preparation of a two-component mixture of the catalytic hydrosilylation is impossible due to poor solubility of components. This cross-linking approach can be applied to obtain new functional materials, in particular, heterogeneous reducing agents^[62] and/or electroactive ferrocene-containing silicone rubbers.

3.2 | Swelling properties

FSR1 and **FSR2** do not dissolve in organic solvents (toluene or benzene) but only swell in them. The density (ρ) of the silicone rubbers was estimated by the pycnometer method for the calculation of the swelling parameters. As expected, there is a correlation between the values of the swelling percentage (s), soluble fraction (w_{sol}), and volume fraction of the polymer in the swollen sample (v). The greatest s and w_{sol} values and the smallest v value are listed for each series of **FSR1** and **FSR2** networks in comparison with those of cross-linked **PMHS** (Table 1). The degree of cross-linking for the ferrocenyl-containing rubbers is 1.5–2.5 times lower than that for the cross-

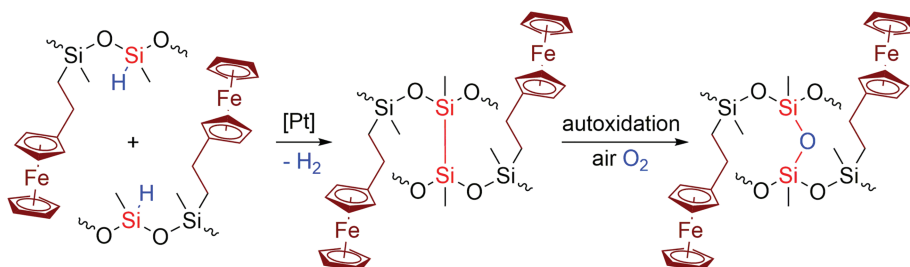
linked **PMHSs**. Obviously, the initial co-polymers **FS1** and **FS2** contain fewer Si–H groups than does **PMHS**. This fact leads to the formation of fewer cross-links between Si–H groups than that when polysiloxane without ferrocene fragments is used.

3.3 | Tensile properties

The elastic properties of **FSR1** and **FSR2** include a relatively higher elongation at break (ε) but a higher tensile strength (σ) than that of samples of the cross-linked **PMHS** (Table 1). For **FSR1** and **FSR2**, the σ values are 0.89 and 0.75 MPa, and the ε values are 130% and 120%, respectively. These results are in agreement with the aforesaid swelling properties. The tensile properties of **FSR1** and **FSR2** are better than those of the **PMHS** cases. The inclusion of ferrocenyl fragments increases the tension of the samples by approximately two to five times and the elongation by up to 25% (in the case of Karstedt's catalyst). However, for the ferrocenyl-containing samples cross-linked using *cis*-[PtCl₂(BnCN)₂], the elongation ε remains almost unchanged compared with that of samples cross-linked using Karstedt's catalyst.

3.4 | Ferrocene content

The molar content of the ferrocenyl-containing unit –OSi(CH₂CH₂Cp₂Fe)CH₃– in **FS1** and **FS2** established by ¹H NMR analysis (the integral ratio Cp₂Fe:SiH = 9.0:1.0, Figure S7, Supporting Information) is approximately 50%.



SCHEME 2 Possible cross-linking ways of ferrocenyl-containing polymethylhydrosiloxanes

TABLE 1 Swelling and tensile properties of the silicone rubbers

Silicone rubber	ρ (g/ml)	s (%)	w_{sol} (%)	ν	ε (%)	σ (MPa)
FSR1	1.11 ± 0.04	195 ± 10	23.4 ± 0.8	0.35 ± 0.01	130 ± 10	0.89 ± 0.07
FSR2	1.11 ± 0.04	198 ± 10	26.4 ± 0.6	0.33 ± 0.01	120 ± 10	0.75 ± 0.06
Cross-linked PMHS^a	1.05 ± 0.04	121 ± 6	0.5 ± 0.1	0.80 ± 0.07	105 ± 5	0.20 ± 0.01
Cross-linked PMHS^b	1.04 ± 0.04	159 ± 8	6.8 ± 0.1	0.54 ± 0.05	110 ± 5	0.47 ± 0.02

^aPMHS cross-linked with Karstedt's catalyst.

^bPMHS cross-linked with *cis*-PtCl₂(BnCN)₂.

PMHS, α,ω -di(trimethylsiloxy)polymethylhydrosiloxane; ρ , density of a silicone rubber; s, swelling percentage of a silicone rubber; w_{sol} , soluble fraction of the swollen polymer; ν , volume fraction of the polymer in the swollen sample; ε , elongation at break; σ , tensile strength.

Because the broad signals of the silicone rubbers in the ¹H SSNMR spectra cannot be integrated correctly, the iron content of **FSR1** and **FSR2** was estimated by energy-dispersive X-ray (EDX) spectroscopy with prior calibration using solutions of ferrocene in **PMHS** within the determined concentration range (Table S1, Supporting Information). The iron content and ferrocene content in the samples are 14.72 ± 0.02 wt.% and 48.91 ± 0.02 wt.%, respectively. Thus, the results of the EDX measurements are in good agreement with the ¹H NMR data of **FS1** and **FS2**.

3.5 | Electrophysical properties and conductivity mechanism

Because the quality of **FSR2** is better than that of **FSR1**, electrophysical studies were performed for only **FSR2**. The electrical resistivity of **FSR2** was studied using broadband impedance spectroscopy, which measures the electrical conductivity of solid materials using a high-frequency current (from 10⁻¹ to 10⁶ Hz). For studying conductivity, **FS2** was directly cross-linked on an electrode, thus making **FSR2** as the most optimal sample (both on cross-linking and electrical conductivity). The cross-linked **PMHS** with *cis*-[PtCl₂(BnCN)₂] and its mixture with 5 wt.% ferrocene (a solid solution of ferrocene at maximum possible concentration in **PMHS**, Figure S1, Supporting Information) were tested as reference samples.

TABLE 2 Electrophysical properties of samples at 25 °C

Silicone rubber	Surface resistivity, $1 \times 10^9 \Omega/\square$	Specific volume resistivity at 1 kHz, $1 \times 10^9 \Omega \text{ cm}$	Specific bulk conductivity at 1 kHz, $1 \times 10^{-9} \text{ S/cm}$
FSR2 (50 wt.% ferrocenyl units)	7	5	3.25
Mixture of PMHS with 5 wt.% ferrocene	20	900	0.98
Cross-linked PMHS	98,000	966	0.74

PMHS, α,ω -di(trimethylsiloxy)polymethylhydrosiloxane.

It has been demonstrated that the surface resistivity of the tested **FSR2** samples was approximately 10⁹ Ω/◻ (Table 2), similar to that of ESD protective materials,^[1,31,63] and is approximately 10,000 more than that of the cross-linked **PMHS**. Comparison of the specific bulk conductivity of **FSR2** with that of reference sample of the cross-linked **PMHS** at 25 °C clearly shows that **FSR2** is more conductive (approximately four times; Figure 2a). Notably, the conductivity of **FSR2** has a metal-like form at a low frequency range up to 10 Hz that remains independent of frequency changes. In addition, at elevated temperatures, the conductivity curves have the same appearance. Specific bulk conductivity of **PMHS** with 5 wt.% ferrocene mixture is almost the same as cross-linked **PMHS** (Table 2).

Broadband dielectric spectroscopy was applied to elaborate details of the conductivity mechanism in **FSR2**. Figure 2b shows the dependence of the imaginary electric modulus part (M'') on the frequency (f) at several temperatures. It can be seen that below 0 °C, the magnitudes and positions of the peaks are nearly constant. As the temperature increases above 0 °C, the maxima shift toward higher frequencies with a simultaneous decrease in magnitude.

At the same time, the masterplot of the normalized imaginary modulus versus normalized frequency (Figure 2c) clearly shows a practically constant shape of the conductivity peak without asymmetry and widening. In our opinion, this behavior of the conductive polymer confirms the material having an electron hopping or

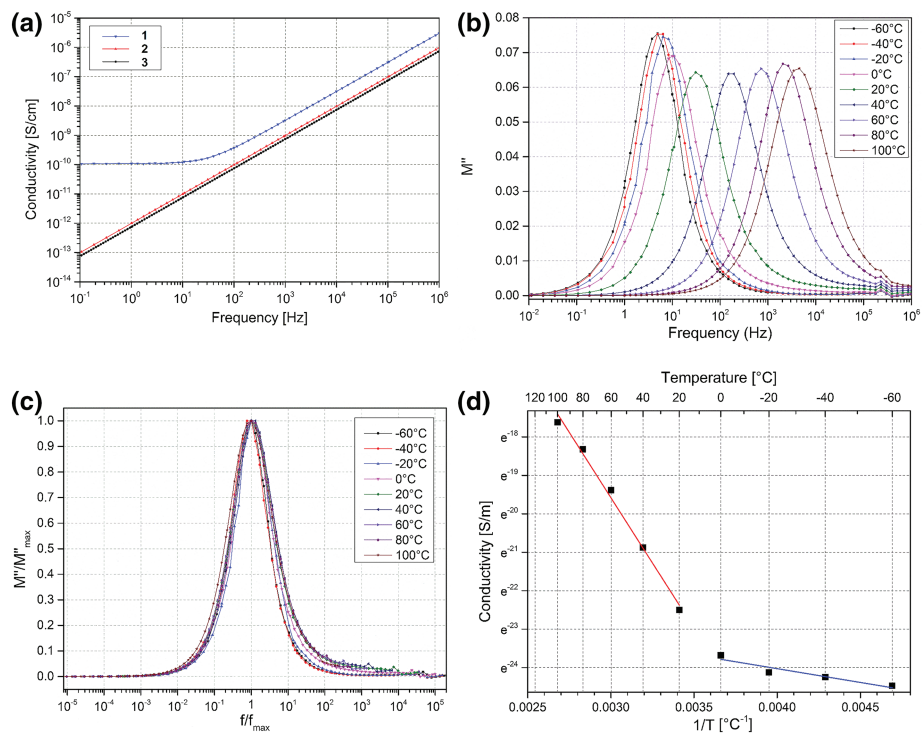


FIGURE 2 Electrophysical properties of the silicone films: (a) the frequency dependence of conductivity at 25 °C: 1, **FSR2**; 2, mechanical mixture of **PMHS** with 5 wt.% ferrocene; 3, cross-linked **PMHS** (without additives); (b) imaginary electric modulus part of **FSR2** at different temperatures; (c) masterplot of normalized imaginary electric modulus part M'' versus normalized frequencies at different temperatures; (d) Arrhenius plot of **FSR2** conductivity against reciprocal temperature. PMHS, α,ω -di(trimethylsiloxy)polymethylhydrosiloxane

tunneling nature^[64–66] of conductivity. The temperature dependence of the M'' maxima can be attributed to increasing charge carrier mobility with heating, and the absence of temperature broadening and asymmetry is characteristic of electronic transfer (compared with ionic conductors and dielectric relaxations).

Arrhenius plots of conductivity versus reciprocal temperature are usually used to estimate the apparent activation energies of thermally dependent processes. The natural logarithm of bulk conductivity (σ) at the M'' maxima is plotted as a function of $1/T$ (Figure 2d), so the slope is proportional to E_{act}/k_B through the following equation:

$$\sigma = \sigma_0 e^{\left(\frac{-E_{act}}{kT}\right)} \quad (2)$$

Two linear regions can be seen on the resulting plot: −60 to 0 °C and 20 to 100 °C, with corresponding activation energies of 0.62 and 5.59 eV, respectively. A sharp increase in the activation energy between 0 and 20 °C can be related to a consequent hopping barrier increase due to higher cross-linked polymer segmental movement. The resulting values are comparable with E_{act} values of pure ferrocene published earlier^[67,68]: 0.61 and 0.60 eV.

4 | CONCLUSIONS

In this study, we realized the synthesis of new self-cross-linked ferrocenyl-containing polymethylhydrosiloxanes. First, it is observed that platinum(0) or (II) species catalyzed the self-cross-linking of **FS1** and **FS2** by reactions between the Si-H groups. The ferrocene content in the obtained silicone rubbers is approximately 50 wt.%.

Second, in comparison with the hyperactive Karstedt's catalyst, *cis*-[PtCl₂(BnCN)₂] demonstrates lower activity and allows the creation of high-quality ferrocenyl-containing silicone rubbers without visible mechanical defects (bubbles and cracks).

Third, compared with the cross-linked polymethylhydrosiloxanes, the cross-linked ferrocenyl-containing polymethylhydrosiloxanes have increased elongation (up to 25%) and tensile strength (up to five times) but have an obviously decreased degree of cross-linking by 1.5–2.5 times.

Fourth, the electrophysical studies show that **FSR2** (50 wt.% ferrocenyl units) has a surface resistivity of approximately $7 \times 10^9 \Omega/\square$, which is an appropriate level for ESD protective materials, and that the conductive polymer exhibits electron tunneling behavior. The surface resistivity of **FSR2** was 10,000 times less than that of pure

polymethylhydrosiloxane ($9.8 \times 10^{13} \Omega/\square$). The synthesis of the ferrocenyl-containing silicone rubbers allows widely varying ferrocene content and increase electrical conductivity unlike mixing PMHS with ferrocene (maximum possible ferrocene concentration is 5 wt.% and surface resistivity is $2 \times 10^{10} \Omega/\square$). These facts support the use of this rubber as an ESD protective material and as an active layer for sensing electronic devices.

ACKNOWLEDGEMENTS

This work was financially supported by the Russian Foundation for Basic Research according to the research project No. 18-33-20062_mol_a_ved. Measurements were performed at the Center for Magnetic Resonance, the Centre for Innovative Technologies of Composite Nanomaterials (all in Saint Petersburg State University).

CONFLICT OF INTEREST

There are no conflicts to declare.

ORCID

Konstantin V. Deriabin  <https://orcid.org/0000-0002-3055-6865>

Ekaterina K. Lobanova  <https://orcid.org/0000-0002-8520-4795>

Sergey O. Kirichenko  <https://orcid.org/0000-0003-3009-7731>

Pavel E. Musienko  <https://orcid.org/0000-0002-7324-9021>

Regina M. Islamova  <https://orcid.org/0000-0003-1180-6539>

REFERENCES

- [1] J. Pionteck, G. Wypych, *Handbook of Antistatics*, Toronto **2016**.
- [2] L. Wang, X. Wang, T. Lin, Conductive coatings for textiles, in *Smart Textile Coatings and Laminates*, Elsevier **2010**.
- [3] N. T. Kakhramanov, K. V. Allahverdiyeva, D. R. Nurullayeva, *Chem. Probl.* **2019**, 17(1), 26.
- [4] W. Zhang, W. Zhang, Z. Xue, Y. Xue, J. Xu, S. Chen, G. Zhang, *J. Mater. Sci.: Mater. Electron.* **2018**, 29(21), 18566.
- [5] P. Pichaimani, S. Krishnan, J. K. Song, A. Muthukaruppan, *High Perform. Polym.* **2018**, 30(5), 549.
- [6] T.E. Hogan, W.L. Hergenrother, M. DeTrano Electrical conductivity of silica-filled rubber compositions using alkali metal salts dissolved in poly (Alkylene Oxide) compounds. US6399692 B2. **2002**.
- [7] O. Hayashida, T. Nakamura Semiconductive silicone rubber composition and silicone rubber roll. US6458859B2. **2002**.
- [8] T. Nakamura, S. Hirabayashi, H. Kikuchi, H. Ando, T. Mizutani Semiconductive silicone rubber compositions and semiconductive silicone rubber rolls. US5725922A. **1998**.
- [9] H. Fujiki, S. Matsubayashi, K. Kanto, T. Suzuki Curable anti-static organopolysiloxane composition and antistatic silicone film. WO2014125826A1. **2014**.
- [10] S. Hirasawa, N. Uchiyama, T. Tojo, T. Uyama, H. Nose, T. Igarashi, Z. Kanzaki Cathode ray tube with conductive silicon adhesive. US5757117A. **1998**.
- [11] L. Wang, Y. Chen, L. Lin, H. Wang, X. Huang, H. Xue, J. Gao, *Chem. Eng. J.* **2019**, 89.
- [12] H. Montazerian, A. Dalili, A. S. Milani, M. Hoofar, *Compos., B Eng.* **2019**, 164, 648.
- [13] D. Chen, Q. Pei, *Chem. Rev.* **2017**, 117(17), 11239.
- [14] K. Wang, G. Ouyang, X. Chen, H. Jakobsen, *Polym. Rev.* **2017**, 57(3), 369.
- [15] S. K. Smoukov, T. Wang, M. Farajollahi, Y. S. Choi, I.-T. Lin, J. E. Marshall, N. M. Thompson, S. Kar-Narayan, J. D. W. Maddden, *Interface Focus* **2016**, 6, 1.
- [16] S. Yao, Y. Zhu, *Adv. Mater.* **2015**, 27(9), 1480.
- [17] G. Kaur, R. Adhikari, P. Cass, M. Bown, P. Gunatillake, *RSC Adv.* **2015**, 5(47), 37553.
- [18] X. Du, X. Hao, Z. Wang, G. Guan, *J. Mater. Chem., A* **2016**, 4(17), 6236.
- [19] C. Zhao, C. Wang, Z. Yue, K. Shu, G. G. Wallace, *ACS Appl. Mater. Interfaces* **2013**, 5(18), 9008.
- [20] M. N. Barshutina, S. O. Kirichenko, V. A. Wodolajski, P. E. Musienko, *Mater. Lett.* **2019**, 236, 183.
- [21] M. Yang, Y. Liang, Q. Gui, J. Chen, Y. Liu, *Mater. Res. Exp.* **2015**, 2(4), 042001.
- [22] J. Vörös, G. Courtine, A. Larmagnac, P. Musienko PDMS-based stretchable multi-electrode and chemotrode array for epidural and subdural neuronal recording, electrical stimulation and drug delivery. EP 2582289B1. **2011**.
- [23] R. M. Islamova, A. V. Vlasov, M. V. Dobrynin, E. A. Masloborodova, E. V. Kaganova, *Russ. J. Gen. Chem.* **2015**, 85(11), 2609.
- [24] R. M. Islamova, M. V. Dobrynin, D. Ivanov, A. V. Vlasov, E. V. Kaganova, G. Grigoryan, V. Y. Kukushkin, *Molecules* **2016**, 21(3), 311.
- [25] R. M. Islamova, M. V. Dobrynin, A. V. Vlasov, A. A. Eremina, M. A. Kinzhakov, I. E. Kolesnikov, A. A. Zolotarev, E. A. Masloborodova, K. V. Luzyanin, *Catal. Sci. Technol.* **2017**, 7(24), 5843.
- [26] K. V. Deriabin, I. A. Yaremenko, M. V. Chislov, F. Fleury, A. O. Terent'ev, R. M. Islamova, *New J. Chem.* **2018**, 42(18), 15006.
- [27] M. V. Dobrynin, C. Pretorius, D. V. Kama, A. Roodt, V. P. Boyarskiy, R. M. Islamova, *J. Catal.* **2019**, 372, 193.
- [28] R. Soltani, A. A. Katbab, *Sensor. Actuat. A Phys.* **2010**, 163(1), 213.
- [29] G. Lüttgens, S. Lüttgens, W. Schubert, *Static Electricity*, Wiley-VCH Verlag GmbH & Co KGaA, Weinheim, Germany, Germany **2017**.
- [30] G. Pritchard, *Plastics Additives: A Rapra Market Report*, Rapra Technology Limited, Shawbury **2005**.
- [31] M. Schiller, *PVC Additives*, Carl Hanser Verlag GmbH & Co, KG, München **2015**.

- [32] C. U. Pittman, *J. Inorg. Organomet. Polym. Mater.* **2005**, 15(1), 33.
- [33] R. Mallick, *Platinum Met. Rev.* **2008**, 52(1), 46.
- [34] B. Alonso, B. González, B. García, E. Ramírez-Oliva, M. Zamora, C. M. Casado, I. Cuadrado, *J. Organomet. Chem.* **2001**, 637–639, 642.
- [35] E. Ospina, M. P. G. Armada, J. Losada, B. Alonso, C. M. Casado, *J. Electrochem. Soc.* **2016**, 163(9), H826.
- [36] C. M. Casado, I. Cuadrado, M. Moran, B. Alonso, M. Barranco, J. Losada, *Appl. Organomet. Chem.* **1999**, 13(4), 245.
- [37] C. Blasco, S. Bruña, I. Cuadrado, E. Delgado, E. Hernández, *Organometallics* **2012**, 31(7), 2715.
- [38] T. Inagaki, H. S. Lee, T. A. Skotheim, Y. Okamoto, *J. Chem. Soc., Chem. Commun.* **1989**, (16), 1181.
- [39] P. Boudjouk, Z. M. H. AL-Badri, B. P. S. Chauhan, *J. Organomet. Chem.* **2004**, 689(21), 3468.
- [40] I. Martínez-Montero, S. Bruña, A. M. González-Vadillo, I. Cuadrado, *Macromolecules* **2014**, 47(4), 1301.
- [41] M. Cazacu, G. Munteanu, C. Racles, A. Vlad, M. Marcu, *J. Organomet. Chem.* **2006**, 691(17), 3700.
- [42] J. Brettar, T. Bürgi, B. Donnio, D. Guillon, R. Klappert, T. Scharf, R. Deschenaux, *Adv. Funct. Mater.* **2006**, 16(2), 260.
- [43] S. Ikeda, N. Oyama, *Anal. Chem.* **1993**, 65(14), 1910.
- [44] O. N. Kadkin, Y. G. Galyametdinov, *Russ. Chem. Rev.* **2012**, 81(8), 675.
- [45] M. Cazacu, A. Vlad, M. Marcu, C. Racles, A. Airinei, G. Munteanu, *Macromolecules* **2006**, 39(11), 3786.
- [46] M. Zamora, S. Bruña, B. Alonso, I. Cuadrado, *Macromolecules* **2011**, 44(20), 7994.
- [47] M. Herrero, B. Alonso, J. Losada, P. García-Armada, C. M. Casado, *Organometallics* **2012**, 31(17), 6344.
- [48] M. Moran, C. M. Casado, I. Cuadrado, J. Losada, *Organometallics* **1993**, 12(11), 4327.
- [49] K. V. Deriabin, E. K. Lobanova-Khaia, A. S. Novikov, R. M. Islamova, *Org. Biomol. Chem.* **2019**, 17(22), 5545.
- [50] V. Y. Kukushkin, M. Tkachuk, N. V. Vorobiov-Desiatovsky, S. Chaloupka, L. M. Venanzi, *Inorg. Synth.* **1998**, 32, 144.
- [51] V. Y. Kukushkin, *Platinum Met. Rev.* **1998**, 42(3), 106.
- [52] K. Plevová, B. Mudráková, R. Šebesta, *Synthesis (Stuttg.)* **2018**, 50(04), 760.
- [53] F. Kremer, A. Schönhals, *Broadband Dielectric Spectroscopy*, Springer, Berlin, Heidelberg **2003**.
- [54] M. Köhler, P. Lunkenheimer, A. Loidl, *Eur. Phys. J. E: Soft Matter Biol. Phys.* **2008**, 27(2), 115.
- [55] E. F. Hairetdinov, N. F. Uvarov, H. K. Patel, *Ferroelectrics* **1996**, 176(1), 213.
- [56] C. T. Moynihan, *J. Non-Cryst. Solids* **1996**, 203, 359.
- [57] R. Anderson, J. Goff, A. Imamura, E. Kimble, G. Lockwood, J. Matisons, Y. Pan, M. Reinert, *Silicon Compounds: Silanes and Silicones. A Survey of Properties and Chemistry*. 3rd edition, Morrisville; **2013**.
- [58] R. Zhang, Z. Zhang, K. Amine, R. West, *Silicon Chem.* **2005**, 2(5–6), 271.
- [59] T. D. Tilley, H.-G. Woo, J. F. Harrod, R. M. Laine, *Inorganic and organometallic oligomers and polymers*, Springer Netherlands, Dordrecht **1991**.
- [60] K. A. Brown-Wensley, *Organometallics* **1987**, 6(7), 1590.
- [61] C. Chatgilialoglu, A. Guerrini, M. Lucarini, G. F. Pedulli, P. Carrozza, G. Da Roit, V. Borzatta, V. Lucchini, *Organometallics* **1998**, 17(11), 2169.
- [62] W. Sun, C. Qian, L. He, K. K. Ghuman, A. P. Y. Wong, J. Jia, A. A. Jelle, P. G. O'Brien, L. M. Reyes, T. E. Wood, A. S. Helmy, C. A. Mims, C. V. Singh, G. A. Ozin, *Nat. Commun.* **2016**, 7, 1.
- [63] J. Paasi, S. Nurmi, R. Vuorinen, S. Strengell, P. Maijala, *J. Electrostat.* **2001**, 51(52), 429.
- [64] D. N. Blauch, J. M. Savéant, *J. Am. Chem. Soc.* **1992**, 114(9), 3323.
- [65] L. Gan, C. S. Suchand Sangeeth, L. Yuan, D. Jańczewski, J. Song, C. A. Nijhuis, *Eur. Polym. J.* **2017**, 97(October), 282.
- [66] R. Pietschnig, *Chem. Soc. Rev.* **2016**, 45(19), 5216.
- [67] B. Mallik, A. Bhattacharjee, *J. Phys. Chem. Solids* **1989**, 50(11), 1113.
- [68] H. Eichhorn, J. Voitländer, *Zeitschrift für Naturforsch. A* **1963**, 18(12), 1373.

SUPPORTING INFORMATION

Additional supporting information may be found online in the Supporting Information section at the end of the article.

How to cite this article: Deriabin KV, Lobanova-Khaia EK, Kirichenko SO, Barshutina MN, Musienko PE, Islamova RM. Synthesis of ferrocenyl-containing silicone rubbers via platinum-catalyzed Si–H self-cross-linking. *Appl Organometal Chem.* 2019;e5300. <https://doi.org/10.1002/aoc.5300>